

Valence-bond crystal in a $\{111\}$ slice of the pyrochlore antiferromagnet

Oleg Tchernyshyov and Hong Yao

Department of Physics and Astronomy, The Johns Hopkins University, Baltimore, Maryland, 21218

R. Moessner

Laboratoire de Physique Théorique de l'Ecole Normale Supérieure, CNRS-UMR8549, Paris, France

We investigate theoretically the ordering effect of quantum spin fluctuations in a Heisenberg antiferromagnet on a two-dimensional network of corner sharing tetrahedra. This network is obtained as a $\{111\}$ slice of the highly frustrated pyrochlore lattice, from which it inherits the equivalence of all three pairs of opposite bonds of each tetrahedron. The lowest-order (in $1/S$) quantum corrections *partially* lift the huge degeneracy of the classical ground state and select an ensemble of states with long-range valence-bond order.

Magnets with strong geometrical frustration have become a focus of experimental studies and inspired a growing number of theoretical inquiries into their unusual properties.¹ For classical spins, strong frustration precludes simple Néel order and creates a vast ground state degeneracy. This degeneracy, in turn, renders the magnet susceptible to nominally small perturbations (dipolar interactions, anisotropies, quantum effects etc.).

An antiferromagnet on the pyrochlore lattice—a network of corner-sharing tetrahedra—is perhaps the ultimate example of strong frustration.^{2,3} Monte Carlo simulations with classical Heisenberg spins show that thermal fluctuations alone are ineffective in restoring magnetic order: the magnet remains in a paramagnetic but correlated state at a temperature as low as $10^{-4}JS^2$. The effect of quantum fluctuations on the pyrochlore antiferromagnet has not yet been determined.

Previous studies have focused on the case of maximal quantum fluctuations, $S = 1/2$. Early on, a ground state in the form of a valence-bond crystal (VBC) was proposed,⁴ which preserves the spin-rotational $O(3)$ symmetry but breaks a number of discrete lattice symmetries, including the equivalence of the three pairs of opposite bonds of a tetrahedron. The relevant local order parameter is constructed from the expectation values $\langle \mathbf{S}_i \cdot \mathbf{S}_j \rangle$. This result was obtained, in the absence (to this day) of a demonstrably reliable analytical treatment, via an uncontrolled approximation; several methods have since yielded similar results.⁵

An alternative route of studying quantum effects begins in the classical limit $S \rightarrow \infty$. At large S , quantum fluctuations are weak and can be evaluated in the framework of a perturbation theory, wherein physical quantities are expanded in powers of $1/S$. The large- S approach has been previously applied to a variety of strongly frustrated magnets.^{6,7,8,9}

In this paper, we report an application of the large- S method to a $\{111\}$ slice of the pyrochlore lattice shown in Fig. 1(a). The resulting lattice can be described as a kagome plane flanked by two triangular lattices, so that every triangle is promoted to a tetrahedron. (Note that this is different from the pyrochlore slab geometry of SCGO,¹⁰ where a triangular lattice is sandwiched be-

tween two kagome planes.)

From the symmetry point of view, our $\{111\}$ slice has the following features important in connection with the pyrochlore in 3D. All its units are equivalent tetrahedra and it thus permits collinear classical ground states (unlike SCGO). Further, unlike the checkerboard version of the 2D pyrochlore,⁹ it retains equivalence between all three pairs of opposing bonds of each tetrahedron, a symmetry spontaneously broken in the $S = 1/2$ pyrochlore VBC mentioned above.⁴

For this lattice, we have found and characterized the subset of classical ground states favored by quantum fluctuations. The problem of minimizing the zero-point energy is equivalent to a discrete gauge-like theory, which by its very nature has many degenerate ground states. A natural first guess is that the ground states are those with uniform flux; this ensemble leads to a semiclassical valence bond liquid. However, our numerical minimisations reveal vacua with a pattern of gauge fluxes violating translational symmetry; this is reflected in a spatial modulation of nearest-neighbor spin correlations $\langle \mathbf{S}_i \cdot \mathbf{S}_j \rangle$. Along with the absence of Néel order, this implies that the spin system is a valence-bond crystal.

We study the Heisenberg spin Hamiltonian

$$H = J \sum_{\langle ij \rangle} \mathbf{S}_i \cdot \mathbf{S}_j = (J/2) \sum_{\alpha} |\mathbf{L}_{\alpha}|^2 + \text{const} = \mathcal{O}(S^2), \quad (1)$$

where $J > 0$ and the sum is taken over all bonds (ij) shown in Fig. 1(a). In the alternative representation, the Greek index α enumerates tetrahedra; \mathbf{L}_{α} is the sum of the four spins residing on tetrahedron α . The energy (1) is minimized when $\mathbf{L}_{\alpha} = 0$ for every tetrahedron α . Classically, this condition does not determine a unique ground state. (This is the hallmark of frustration.) Rather, it defines an enormous manifold of classical vacua. By explicit construction, or Maxwellian counting,³ the dimension of the manifold can be seen to equal twice the number of tetrahedra. Thermal order by disorder is absent.

Quantum fluctuations produce virtual excitations out of the ground state, thereby lowering the vacuum energy. For large S , the quantum correction can be expanded in powers of $1/S$ by expressing the spin operators in terms of Holstein-Primakoff bosons. (The virtual excitations

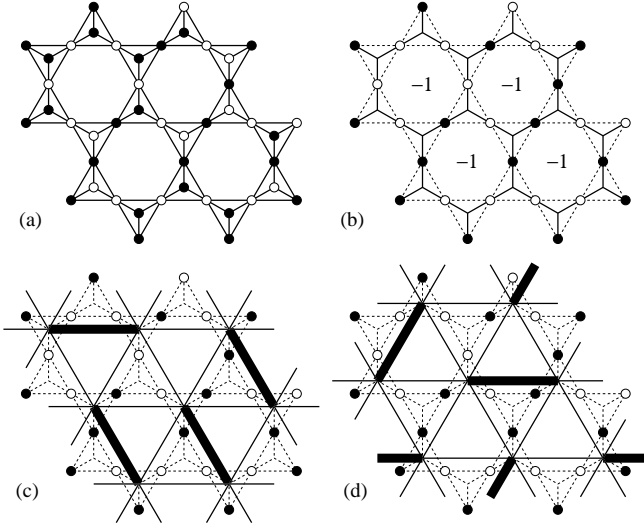


FIG. 1: (a) A generic collinear ground state of Eq. (1) on the pyrochlore slice. Open (filled) dots correspond to $s_i = +1$ (-1). (b) Kagome sites live on links of a honeycomb lattice. The Z_2 flux is -1 through every hexagon. (c) and (d) Resulting dimer coverings of the two triangular sublattices. The dimers cross frustrated bonds ($s_i = s_j$).

are magnon pairs produced by the operators $b_i^\dagger b_j^\dagger$ in the bosonized Hamiltonian.) The lowest-order correction is the zero-point energy of harmonic spin waves,

$$E^{(1)} = -2NJS + \sum_a \hbar|\omega_a|/2 = \mathcal{O}(S), \quad (2)$$

where $\{\omega_a\}$ is the set of spin-wave frequencies in a given classical ground state and N is the number of tetrahedra. The first quantum correction (2) depends implicitly (through the magnon spectrum) on the spin configuration and thus can be viewed as an effective spin potential breaking the degeneracy of the ground-state manifold.

Typically, quantum fluctuations select collinear ground states,¹¹ provided that such vacua exist at the classical level. Although we are unaware of any general proof of this proposition, a compelling argument in its favor can be stated nonetheless. Given that the reduction of the vacuum energy is due to generation of virtual magnon pairs and that magnons are transverse excitations, the zero-point energy should be lower when more adjacent spins share both of their transverse directions, i.e. when spins are collinear. In certain cases this heuristic argument can be made precise.^{7,9,12} We assume that it applies in this case as well and minimize the zero-point energy in the set of collinear classical vacua. As a quick check, we have computed zero-point energies of a few simple classical vacua with the smallest magnetic unit cell, and found them to be $-1.2126JS$, $-1.1612JS$, and $-1.1436JS$ for the collinear, “perpendicular,” and “antiferromagnetic” states, respectively (notation of Ref. 11).

We parametrize collinear states by means of Ising variables $s_i = \pm 1$ such that $\mathbf{S}_i/S = s_i \hat{\mathbf{n}}$, where $\hat{\mathbf{n}}$ is a unit

vector. The constraint of zero total spin on every tetrahedron carries over to the Ising variables: $s_0 + s_1 + s_2 + s_3 = 0$. We can eliminate the variable s_0 on the out-of-plane site at the expense of introducing another constraint:

$$s_1 + s_2 + s_3 = \pm 1 \text{ on every triangle.} \quad (3)$$

It follows from Eq. (3) that collinear classical vacua of the pyrochlore slice can be mapped onto the ground states of a kagome Ising antiferromagnet. Redundancy of the out-of-plane Ising variables allows us to speak interchangeably of triangles and tetrahedra when we deal with ground-state configurations.

The zero-point energy (2) is an implicit function of the Ising variables $\{s_i\}$. As outlined in Refs. 3 and 9, the spin-wave spectrum can be obtained by linearizing the classical equations of motion for the spins, written in terms of the \mathbf{L} variables: $\hbar \dot{\mathbf{L}}_\alpha = \sum_\beta \mathbf{S}_{\alpha\beta} \times \mathbf{L}_\beta$. Here $\mathbf{S}_{\alpha\beta}$ denotes the spin shared by tetrahedra α and β . (All of these spins reside in the kagome plane.) For a collinear spin state polarized along $\hat{\mathbf{n}} = (0, 0, 1)$, transverse fluctuations of the total spin on tetrahedron α can be parametrized by a complex number σ_α as $\mathbf{L}_\alpha = (\text{Re}\sigma_\alpha, \text{Im}\sigma_\alpha, 0)$. The magnon frequencies are then determined by solving the eigenvalue problem

$$JS \sum_\beta s_{\alpha\beta} \sigma_\beta = \hbar\omega \sigma_\alpha. \quad (4)$$

The zero-point energy can now be minimized numerically, e.g. by using simulated annealing. However, it turns out that the states minimizing Eq. (2) retain a large residual degeneracy. Hence, finding one such state does not yet solve the problem. We must first understand the nature of the residual degeneracy. This is best done by discussing a hidden symmetry responsible for it.

A gauge-like symmetry. Observe that the triangles $\{\alpha\}$ occupy the sites of a honeycomb lattice dual to the kagome [Fig. 1(b)]. The in-plane sites $\{\alpha\beta\}$ live on links of the dual lattice. It was noted by Henley¹³ that Eq. (4) reveals a special gauge-like symmetry of the zero-point energy (2). Namely, a transformation

$$\sigma_\alpha \mapsto \sigma'_\alpha = \Lambda_\alpha \sigma_\alpha, \quad s_{\alpha\beta} \mapsto s'_{\alpha\beta} = \Lambda_\alpha s_{\alpha\beta} \Lambda_\beta^{-1} \quad (5)$$

leaves Eq. (4) invariant. (Conservation of Ising spin length $|s_{\alpha\beta}|$ requires that $\Lambda_\alpha = \pm 1$.) Therefore, two spin configurations $\{s_{\alpha\beta}\}$ and $\{s'_{\alpha\beta}\}$ related by the gauge symmetry (5) have identical magnon spectra and, consequently, equal zero-point energies. We therefore expect a large residual degeneracy of the ground state even after the inclusion of the first quantum correction (2).

A word of caution. Transformation (5) is not exactly a gauge symmetry, even though it strongly resembles one. The transformed state must respect the ground-state constraint (3). The importance of this restriction is evident when one ponders the meaning of the transformation: if $\Lambda_\alpha = -1$, we flip *all* Ising spins on triangle α . Doing so may violate the ground-state constraint

(3) on adjacent triangles, where only one spin is flipped. This reduces the number of possible gauge transformations but—crucially—does not eliminate them entirely.

The uncovering of a hidden symmetry greatly simplifies our task: as soon as we find a single ground state minimizing the zero-point energy (2), we can generate all of the others by applying the gauge transformations (5). But the gauge-like symmetry is useful in more ways than one. It also puts restrictions on the way in which the zero-point energy depends on the Ising spin variables.

From the viewpoint of the Z_2 symmetry (5), the Ising spins $s_{\alpha\beta}$ are gauge variables. In a true gauge theory, the energy can only depend on their gauge-invariant combinations, in this instance the Z_2 fluxes through closed loops Γ_ℓ of various lengths ℓ on the hexagonal lattice, $\phi_{\gamma_\ell} = s_{\alpha_1\alpha_2} s_{\alpha_2\alpha_3} \dots s_{\alpha_\ell\alpha_1}$. The flux through any such loop can be factored into a product of fluxes piercing elementary plaquettes of the dual lattice, the hexagons $\gamma = \Gamma_6$ [Fig. 1(b)]. Therefore, the zero-point energy will be a function of Z_2 fluxes:

$$E_1 = E_1(\{\phi_\gamma\}). \quad (6)$$

While ours is not precisely a gauge theory, Eq. (6) is the right guess: *the zero-point energy is entirely determined by the values of the Z_2 fluxes*. To prove this, we demonstrate that any two collinear ground states with the same set of flux variables $\{\phi_\gamma\}$ have equal zero-point energies (2). To accomplish that, we show that the two states are related by a gauge-like transformation (5).

Proof. Let the Ising link variables be $\{s_{\alpha\beta}\}$ and $\{s'_{\alpha\beta}\}$ in the two states. Define new link variables as their ratio, $t_{\alpha\beta} = s'_{\alpha\beta}/s_{\alpha\beta} = \pm 1$. The variables $t_{\alpha\beta}$ are pure gauge: their product along any closed loop equals +1. Therefore we can unambiguously define a new variable Λ_α on sites of the dual lattice in such a way that $\Lambda_\alpha = t_{\alpha\beta}\Lambda_\beta$ everywhere. Hence $s'_{\alpha\beta} = \Lambda_\alpha s_{\alpha\beta} \Lambda_\beta^{-1}$. By Eq. (5), the zero-point energies of the two states are equal. Q.E.D.

The precise form of the flux potential is not fixed by Eq. (6) and can be rather complicated. One might hope that a series expansion could successfully mimic it:

$$\frac{E_1}{N} = a_0 + \frac{1}{N} \sum_{\gamma} a_1 \phi_\gamma + \frac{1}{2N^2} \sum_{\gamma, \gamma'} a_2(\gamma, \gamma') \phi_\gamma \phi_{\gamma'} + \dots \quad (7)$$

If the linear term dominates, the ground state has uniform flux $\phi_\gamma = -\text{sign}(a_1)$ on all elementary plaquettes. On the checkerboard, $\phi_\gamma = +1$ in the ground state.⁹

Extending the same simplistic approach to the pyrochlore slice we can take a guess that the ground states will either have no flux ($\phi_\gamma = +1$) or have the maximal flux π ($\phi_\gamma = -1$). While neither of these is the correct answer, they are interesting in their own right.

The π -flux states. In these ground states, the product of six Ising spins around any hexagon (of the original kagome lattice) equals -1 [Fig. 1(a)]. The π flux on the hexagon is related to the number of frustrated bonds. (A bond is frustrated if it connects Ising spins $s_i = s_j$.)

More precisely, each hexagon has 0 or 2 frustrated bonds belonging to the triangles pointing *down* [Fig. 1(b)]. This fact allows us to map any π -flux state onto a dimer covering. If a hexagon has 2 such frustrated bonds, draw a dimer connecting the centers of the two triangles contributing the frustrated bonds [Fig. 1(c)]. Because every triangle has exactly one frustrated bond, it shares a dimer with one other triangle. The same construction applies to the sublattice of triangles pointing up [Fig. 1(d)]. We note that gauge transformations on the down triangles are sufficient to take any of the dimer states on the up triangles into any other without changing the dimer state on the down triangles – and vice versa. Thus every π -flux ground state maps onto a pair of *completely independent* dimer coverings of the triangular lattices.

Now one can use the well-known properties of the dimer model on the triangular lattice¹⁴ to characterize the ensemble of the π -flux states. By construction, the number of such states equals the number of pairs of dimer coverings. The latter grows exponentially with the number of sites, so that there is a finite entropy of 0.4286 per tetrahedron. A disordered state of classical dimers on a triangular lattice translates into the absence of valence-bond order in our spin model. Spin correlations are also short-ranged. On a lattice with periodic boundary conditions (on a torus), these ground states fall into four disconnected topological classes distinguished by the values of the global Z_2 fluxes piercing the torus.

In short, the ensemble of π -flux states describes a classical valence-bond liquid.

The actual ground states. We have performed a numerical minimization of the zero-point energy (2) in the space of collinear vacua (3) using the method of simulated annealing. A Monte Carlo step, conserving the classical energy (1), consisted of flipping a randomly chosen chain of alternating spins. The zero-point energy (2) was then determined numerically.

Initial runs were done on systems containing between 100 and 200 tetrahedra. Starting from a periodic state we randomized the system by flipping randomly chosen antiferromagnetic chains until spin correlations with the original state were lost. The lattice was then annealed to achieve a state with the lowest energy. Throughout a simulation, we monitored Ising spins s_i , valence-bond variables $s_i s_j$, and Z_2 fluxes on hexagons. The low-energy states obtained by the annealing showed no apparent spin or valence-bond order [Fig. 2(a)]. However, the Z_2 fluxes showed a clear tendency to order: 1/4 quarter of the hexagons had the trivial Z_2 flux +1 and formed a regular pattern [Fig. 2(a)]. We denote such states as 2×2 after the size of the unit cell.

Finite-size scaling studies (with up to 10^4 tetrahedra) yielded the zero-point energies of $-1.2127JS$, $-1.2462JS$, and $-1.2497JS$ per tetrahedron for the no-flux, π -flux, and 2×2 states, respectively, with the 2×2 states the lowest. On the basis of the energy differences, we estimate that quantum selection of ground states will be effective below the temperature scale of roughly

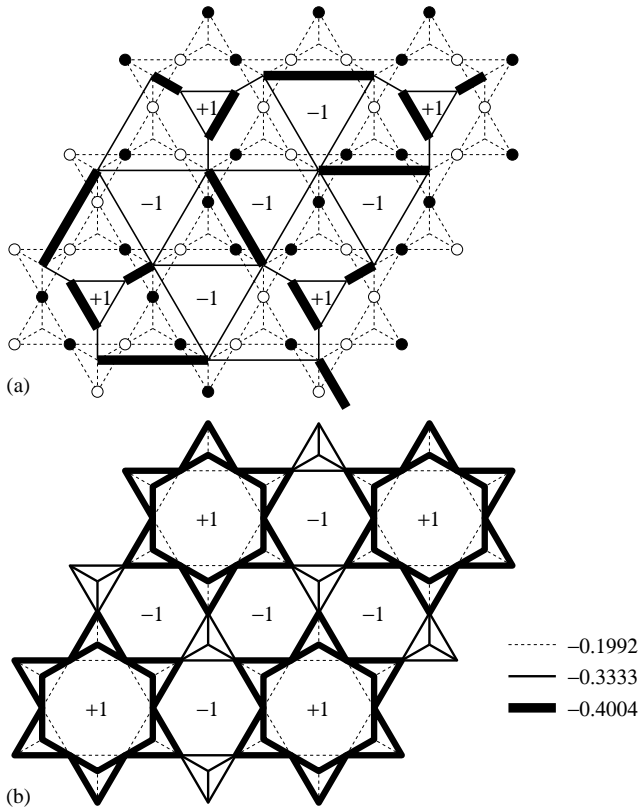


FIG. 2: (a) A generic 2×2 collinear ground state and the corresponding dimer covering (only one dual sublattice is shown). Solid lines depict the decorated triangular lattice. The numbers ± 1 indicate the \mathbb{Z}_2 flux. (b) Expectation values of the valence-bond variables $\langle s_i s_j \rangle$ are encoded in line thickness.

$10^{-2}JS/k_B$. Note that the naïve energy scale JS comes with a numerically small prefactor.

To obtain a dimer model appropriate for the 2×2 flux pattern, we start with the dimers on a triangular lattice, which yield the π -flux states [Fig. 1(c)]. To change the

flux from -1 to $+1$ on one quarter of the hexagons, we decorate the triangular lattice by modifying one quarter of triangles [Fig. 2(a)]. Again, every frustrated bond is intersected by a dimer.

The properties of classical dimers on the decorated lattice can be readily computed by using Grassmann variables. The number of 2×2 ground states is exponentially large, with an entropy per tetrahedron of 0.4248. The probability to find a dimer on a short link is $p = 0.4004 > 1/3$. In spin language this means that $\langle s_i s_j \rangle = p(+1) + (1-p)(-1) = -0.1992 > -1/3$ on links surrounding the hexagons marked $+1$. These bonds are therefore more frustrated than the lattice average. On the other hand, a tetrahedron placed symmetrically with respect to the three closest fluxes $+1$ has $\langle s_i s_j \rangle = -1/3$ for all its bonds. The valence-bond averages $\langle s_i s_j \rangle$ are shown schematically in Fig. 2(b). They are nonuniform, therefore the ensemble of 2×2 states has valence-bond order that enlarges the lattice unit cell. (We note in passing a similarity with the valence-bond order proposed earlier for the three-dimensional $S = 1/2$ pyrochlore:^{4,5} $3/4$ of tetrahedra have unequal valence-bond correlations; the other $1/4$ remain symmetric.)

Spin correlations $\langle s_i s_j \rangle$ between more distant neighbors decay exponentially with distance. The correlation length is 1.15 (the unit of length is the side of a tetrahedron). This points to the absence of Néel order.

To summarize, we find that, to leading order in $1/S$, quantum fluctuations select a collinear ensemble of degenerate ground states with additional bond order and no spin order: we have a valence-bond crystal. This degeneracy may be lifted in higher orders in $1/S$, as found previously for the Heisenberg antiferromagnet on kagome.^{15,16}

The authors thank A.G. Abanov, C. Broholm, C.L. Henley, S.L. Sondhi, and O.A. Starykh for useful discussions. R. M. was supported in part by the Ministère de la Recherche et des Nouvelles Technologies.

¹ P. Schiffer and A. P. Ramirez, Comments Cond. Mat. Phys. **18**, 21 (1996); M.J. Harris and M.P. Zinkin, Mod. Phys. Lett. B **10**, 417 (1996); J.E. Greedan, J. Mater. Chem. **11**, 37 (2001); R. Moessner, Can. J. Phys. **79**, 1283 (2001).
² P. W. Anderson, Phys. Rev. **102**, 1008 (1956); J. Villain, Z. Phys. B **33**, 31 (1979).
³ R. Moessner and J.T. Chalker, Phys. Rev. Lett. **80**, 2929 (1998); Phys. Rev. B **58**, 12049 (1998).
⁴ A. B. Harris, A.J. Berlinsky, and C. Bruder, J. Appl. Phys. **69**, 5200 (1991).
⁵ H. Tsunetsugu, J. Phys. Soc. Japan **70**, 640 (2001); A. Koga and N. Kawakami, Phys. Rev. B **63**, 144432 (2001); E. Berg, E. Altman, and A. Auerbach, Phys. Rev. Lett. **90**, 147204 (2003).
⁶ J.T. Chalker, P.C.W. Holdsworth, and E.F. Shender, Phys. Rev. Lett. **68**, 855 (1992).
⁷ T. Yildirim, A.B. Harris, and E.F. Shender, Phys. Rev. B **53**, 6455 (1996).

⁸ R.R. Sobral and C. Lacroix, Sol. State Comm. **103**, 407 (1997).
⁹ O. Tchernyshyov, O. Starykh, R. Moessner, and A.G. Abanov, Phys. Rev. B **68**, 144422 (2003).
¹⁰ X. Obradors *et al.*, Solid State Commun. **65**, 189 (1988); A.P. Ramirez, G.P. Espinosa, and A.S. Cooper, Phys. Rev. Lett. **64**, 2070 (1990).
¹¹ C.L. Henley, J. Appl. Phys. **61**, 3962 (1987).
¹² M. Biskup, L. Chayes, and S.A. Kivelson, math-ph/0310001.
¹³ C.L. Henley (unpublished). See Ref. 9 for an outline.
¹⁴ P. Fendley, R. Moessner, and S.L. Sondhi, Phys. Rev. B **66**, 214513 (2002).
¹⁵ A. Chubukov, Phys. Rev. Lett. **69**, 832 (1992).
¹⁶ C.L. Henley and E.P. Chan, J. Mag. Mag. Mater. **140-144**, 1693 (1995).